ChemComm

Chemical Communications

A Rigid Donor-Acceptor Daisy Chain Dimer

Dennis Cao,[a,b] Cheng Wang,[a] Marc Giesener,[a] Zhichang Liu,[a] and J. Fraser Stoddart*[a,b]

[a] *Department of Chemistry, Northwestern University, 2145 Sheridan Road, Evanston, Illinois 60208, United States.*

[b] *NanoCentury KAIST Institute and Graduate School of EEWS (WCU), Korea Advanced Institute of Science and Technology (KAIST)373−1, Guseong Dong, Yuseong Gu, Daejeon 305−701, Republic of Korea.*

SUPPORTING INFORMATION

Table of Contents

S1. General Methods

All reagents and starting materials were purchased from Aldrich and used without further purification. Compounds **2**,[S1] **6**,[S2] **10**,[S3] and **S2**•4PF_6[S4] were prepared according to literature procedures. All reactions were performed under an N_2 atmosphere and in dry solvents unless otherwise stated. Column chromatography was carried out using silica gel 60 as the stationary phase. High Performance Liquid Chromatography (HPLC) purification was carried out on a preparative reverse phase-HPLC (RP-HPLC) instrument, using a C18 column. UV-Vis spectra were recorded on a Varian 100-Bio UV/Vis spectrophotometer. 1D and 2D nuclear magnetic resonance (NMR) spectra were recorded on Bruker Avance III 500 and 600 MHz spectrometers. Chemical shifts in the ^{1}H NMR spectra are reported in ppm relative to the signals corresponding to the residual non-deuterated solvent. Chemical shifts are reported in ppm relative to the signals corresponding to the residue non-deuterated solvents ($CDCl_3$: δ 7.26 ppm, CD_3CN: δ 1.94 ppm, CD_3COCD_3: δ 2.05 ppm, CD_3SOCD_3: δ 2.50 ppm). The following abbreviations are used to explain the multiplicities: s, singlet; d, doublet; t, triplet; b, broad peaks; m, multiplet or overlapping peaks. High resolution electrospray ionization mass spectra (HRMS-ESI) were measured on an Agilent 6210 LC-TOF with Agilent 1200 HPLC introduction. High-resolution nano-assisted laser desorption/ionization (NALDI) mass spectra were measured on a Bruker Autoflex III mass spectrometer.

S2. Synthetic Procedures

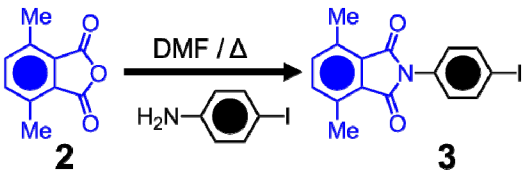

Figure S1: Synthesis of **3**.

2: 2,5-Dimethylphthalic anhydride[S1] (3.00 g, 17.1 mmol) and *p*-iodoaniline (4.48 g, 20.5 mmol) were dissolved in DMF (200 mL) and heated at 120 °C overnight. After cooling to RT, the reaction mixture was concentrated by rotary evaporation. The residue was dissolved in CH_2Cl_2 and washed with 2M HCl and brine. The organic layer was then dried ($MgSO_4$), filtered, and concentrated to yield **2** as a tan-yellow solid (6.07 g, 94%). M.p. 145−146 °C; ^{1}H NMR ($CDCl_3$,

500MHz, 298 K): δ = 7.82 (d, *J* = 8.6 Hz, 2H), 7.40 (s, 2H), 7.20 (d, *J* = 8.6 Hz, 2H), 2.69 (s, 6H); ^{13}C NMR ($CDCl_3$, 125 MHz, 298 K): δ = 167.6, 138.1, 136.6, 136.1, 131.6, 128.4, 128.4, 93.0, 17.6; HRMS (ESI+): calcd for $[M + H]^+$ *m/z* = 377.9985; found *m/z* = 377.9986.

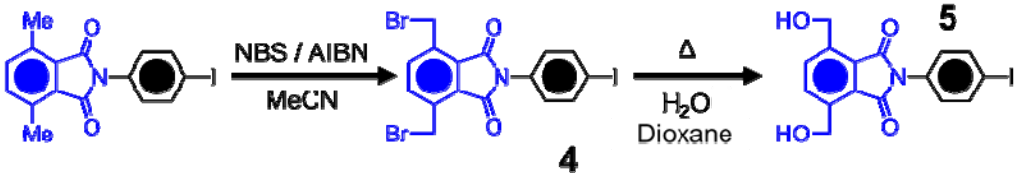

Figure S2: Synthesis of **4** and **5**.

5: The iodide **3** (5.52 g, 14.6 mmol), NBS (10.4 g, 58.6 mmol), and AIBN (120 mg, 0.7 mmol) were added to dry MeCN (200 mL) and the reaction mixture was heated under reflux for 8 h. The reaction was monitored by TLC and the mixture cooled to RT upon the disappearance of **3**. The crude product was subjected to chromatography (CH_2Cl_2/Hexanes 1:4) to separate the tri- and tetrabrominated products from the mono- and dibrominated ones. The mixture (3.3 g) of mono- and dibromo compounds was then added to dioxane/H_2O (300 mL, 1/1) and the reaction mixture was heated under reflux overnight. After cooling to RT, the reaction mixture was diluted with H_2O and extracted with CH_2Cl_2. The organic layer was then washed with $NaHCO_3$ and brine, dried ($MgSO_4$), and concentrated to yield a crude mixture of the alcohol and the diol. The crude product was washed through a plug of silica with CH_2Cl_2 to remove the alcohol before the column was eluted with EtOAc to isolate the desired diol **5** as a white, feathery solid (722 mg, 12%) containing ~7% of the product in which the iodine has been exchanged with bromine. M.p. 179−181 °C; ^{1}H NMR (CD_3COCD_3, 500 MHz, 298 K): δ = 8.03 (s, 2H), 7.92 (d, *J* = 8.6 Hz, 2H), 7.34 (d, *J* = 8.6 Hz, 2H), 5.12 (s, 4H), 4.59 (t, *J* = 5.7 Hz, 2H); ^{13}C NMR (CD_3COCD_3, 125 MHz, 298 K): δ = 168.2, 141.8, 141.7, 138.8, 133.3, 130.1, 128.0, 93.3, 60.3; HRMS (ESI+): calcd for $[M + Na]^+$ *m/z* = 431.9703; found *m/z* = 431.9704.

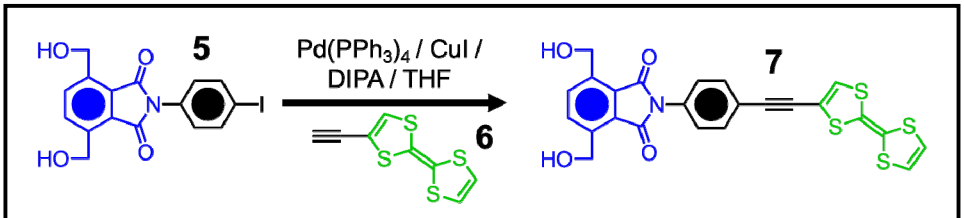

Figure S3: Synthesis of **7**.

7: Freshly prepared ethynyltetrathiafulvalene[S2] **6** (415 mg, 1.8 mmol), **5** (500 mg, 1.2 mmol), CuI (23 mg, 0.1 mmol), and diisopropylamine (1 mL, 7 mmol) were dissolved in dry THF (125

mL). After degassing the solution for 20 min with N_2, $Pd(PPh_3)_4$ (43 mg, 0.04 mmol) was added. The reaction mixture was heated at 60 °C under N_2 protection overnight before being cooled to RT and concentrated by rotary evaporation. The residue was subjected to chromatography (CH_2Cl_2 → CH_2Cl_2/EtOAc 3/1) to yield **7** as a red solid (535 mg, 86%). M.p. ~180 °C decomp.; ^{1}H NMR (CD_3COCD_3, 500 MHz, 298 K): δ = 8.04 (s, 2H), 7.68 (d, *J* = 8.6 Hz, 2H), 7.59 (d, *J* = 8.6 Hz, 2H), 7.06 (s, 1H), 6.69 (s, 1H), 6.68 (s, 1H), 5.12 (s, 4H), 4.59 (br s, 2H); ^{13}C NMR (CD_3COCD_3, 125 MHz, 298 K): δ = 168.2, 141.8, 138.8, 134.0, 133.3, 132.7, 128.1, 128.0, 127.6, 121.8, 120.6, 120.3, 115.6, 114.5, 93.3, 81.7, 60.3; HRMS (ESI+): calcd for $[M]^{*+}$ *m/z* = 508.9878; found *m/z* = 508.9878.

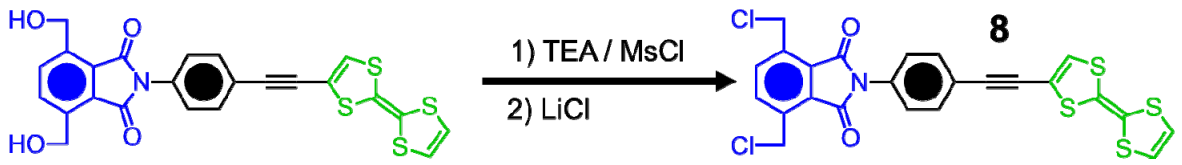

Figure S4: Synthesis of **8**.

8: The diol **7** (500 mg, 0.9 mmol) was dissolved in THF (50 mL) and the solution was degassed for 20 min with N_2. TEA (1.8 mL, 13 mmol) and MsCl (1.2 mL, 16 mmol) were added to this solution at RT. After 30 min, LiCl (3 g, 70.7 mmol) was added and the reaction mixture degassed for 20 min with N_2 before being stirred overnight under N_2. H_2O was added to the reaction mixture and the aqueous solution was extracted with CH_2Cl_2. The organic layer was washed with H_2O, dried ($MgSO_4$), filtered, and concentrated. The residue was subjected to chromatography (CH_2Cl_2/Hexanes 1/2 → CH_2Cl_2) to yield a red-brown solid (229 mg, 43%). M.p. ~175 °C decomp.; ^{1}H NMR (CD_3COCD_3, 500 MHz, 298 K): δ = 8.05 (s, 2H), 7.71 (d, *J* = 8.6 Hz, 2H), 7.63 (d, *J* = 8.6 Hz, 2H), 7.07 (s, 1H), 6.69 (s, 1H), 6.68 (s, 1H), 5.24 (s, 4H); ^{13}C NMR (CD_3SOCD_3, 125 MHz, 298 K): δ = 165.9, 136.3, 136.3, 132.3, 131.9, 128.5, 128.3, 127.7, 120.5, 120.2, 120.0, 113.9, 113.4, 105.5, 92.4, 81.1, 39.6; MS (NALDI-TOF): calcd for [*M*] *m/z* = 546.921; found *m/z* = 546.902.

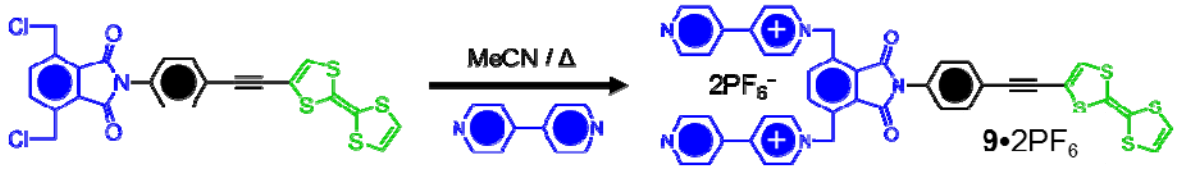

Figure S5: Synthesis of **9**•2PF_6.

9•2PF$_6$: Dichloride **8** (215 mg, 0.4 mmol) and 4,4'-bipyridine (1.5 g, 9.6 mmol) were dissolved in dry MeCN (100 mL). NaBr (634 mg, 6.2 mmol) was added to this solution. The reaction mixture was degassed for 20 min with N_2 before being heated under reflux for 48 h under N_2, during which time a brown precipitate formed. After cooling to RT, the solid was collected by filtration and dissolved in MeOH. Addition of aq. NH_4PF_6 precipitated **9**·2PF$_6$ as a brown solid (338 mg, 86%). M.p. ~215 °C decomp.; ^{1}H NMR (CD_3CN, 500 MHz, 298 K): δ = 8.89 (d, *J* = 7.0 Hz, 4H), 8.84 (d, *J* = 7.0 Hz, 4H), 8.31 (d, *J* = 7.0 Hz, 4H), 8.04 (s, 2H), 7.77 (d, *J* = 7.0 Hz, 4H), 7.64 (d, *J* = 8.6 Hz, 2H), 7.40 (d, *J* = 8.6 Hz, 2H), 6.84 (s, 1H), 6.50 (s, 2H), 6.19 (s, 4H); ^{13}C NMR (CD_3CN, 125 MHz, 298 K): δ = 166.1, 154.6, 150.8, 145.3, 140.7, 137.2, 131.9, 131.8, 131.2, 130.5, 126.8, 126.7, 125.6, 121.5, 119.3, 119.2, 114.1, 106.0, 91.8, 81.0, 58.5; HRMS (ESI+): calcd for $[M - PF_6]^+$ *m/z* = 932.084; found *m/z* = 932.0852.

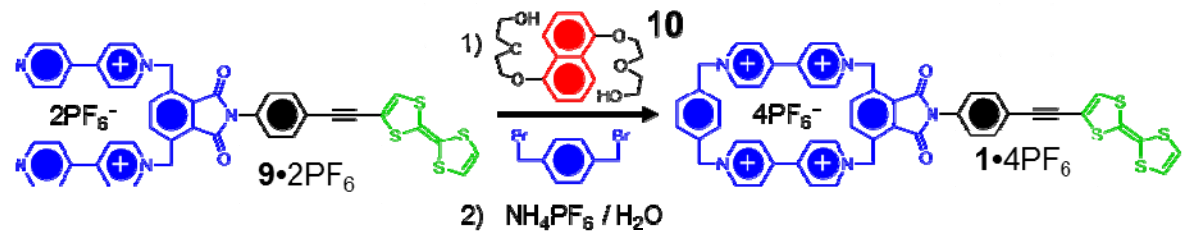

Figure S6: Synthesis of **1**•4PF$_6$.

1•4PF$_6$: **9**•2PF$_6$ (200 mg, 0.2 mmol), 1,4-bis(bromomethyl)benzene (59 mg, 0.2 mmol), and **10**[S3] (288 mg, 0.9 mmol) were dissolved in dry DMF (50 mL) and stirred under N_2 for 1 week. After removing the solvents under reduced pressure, the resulting mixture was purified by HPLC (H_2O−MeCN, 0−60% in 20 min, λ = 254 nm) to yield **1**·4PF$_6$ as a green solid (23 mg, 8 %) after counterion exchange with NH_4PF_6. M.p. ~220 °C decomp.;^{1}H NMR (CD_3CN, 500 MHz, 333 K): δ = 8.94 (d, J = 6.7 Hz, 4H), 8.85 (d J = 6.7 Hz, 4H), 8.20 (d, *J* = 6.8 Hz, 4H), 8.16 (s, 2H), 8.15 (d, *J* = 6.7 Hz, 4H), 7.66 (d, *J* = 8.4 Hz, 2H), 7.44 (s, 4H), 7.43 (d, *J* = 8.4 Hz, 2H), 6.84 (s, 1H), 6.51 (s, 2H), 6.24 (s, 4H), 5.76 (s, 4H); HRMS (ESI+): calcd for $[M - PF_6]^+$ *m/z* = 1326.075; found *m/z* = 1326.0789 calcd for $[2M - PF_6]^+$ *m/z* = 2797.1153; found *m/z* = 2797.1162.

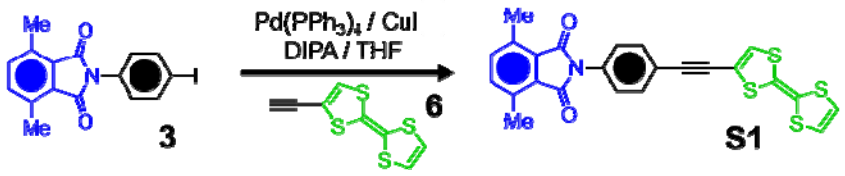

Figure S7: Synthesis of **S1**.

S1: Freshly prepared ethynyltetrathiafulvalene **6** (120 mg, 0.5 mmol), **3** (200 mg, 0.5 mmol), CuI (10 mg, 0.05 mmol), and diisopropylamine (0.4 mL, 3 mmol) were dissolved in dry THF (50 mL). After degassing the solution for 20 min with N_2, $Pd(PPh_3)_4$ (43 mg, 0.02 mmol) was added. The reaction mixture was heated at 60 °C under N_2 overnight. It was cooled to RT and concentrated by rotary evaporation. The residue was subjected to chromatography (CH_2Cl_2) to yield **S1** as a red solid (129 mg, 51%). ^{1}H NMR (CD_3COCD_3, 500 MHz, 298 K): δ = 7.68 (d, *J* = 8.6 Hz, 2H), 7.59 (d, *J* = 8.6 Hz, 2H), 7.54 (s, 2H), 7.06 (s, 1H), 6.69 (s, 1H), 6.68 (s, 1H), 2.66 (s, 6H); ^{13}C NMR (CD_3COCD_3, 125 MHz, 298 K): δ = 137.4, 136.5, 132.7, 129.5, 128.1, 127.5, 120.6, 120.3, 90.5, 79.8, 17.5.

S3. ^{1}H NMR and UV-Vis Spectroscopy of Model Compound S1

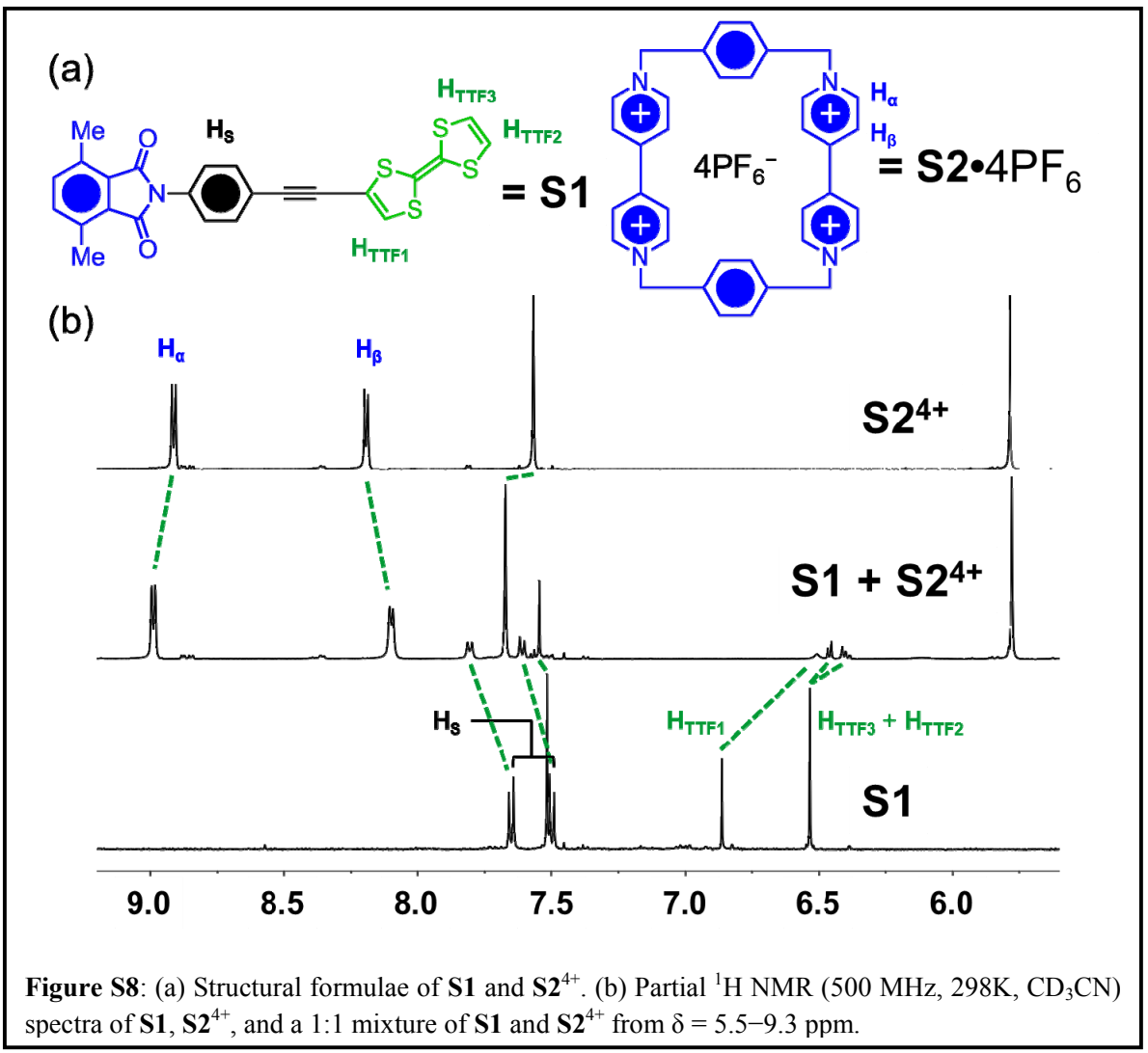

Figure S8: (a) Structural formulae of **S1** and **S2**$^{4+}$. (b) Partial ^{1}H NMR (500 MHz, 298K, CD_3CN) spectra of **S1**, **S2**$^{4+}$, and a 1:1 mixture of **S1** and **S2**$^{4+}$ from δ = 5.5−9.3 ppm.

S1 was synthesised as a model compound to evaluate whether or not the addition of the phenylacetylene spacer to the tetrathiafulvalene (TTF) unit would inhibit its binding interactions with $CBPQT^{4+}$ (**S2**$^{4+}$). When **S1** and **S2**•$4PF_6$ are mixed together in a 1:1 ratio, large changes occur in the ^1H NMR spectrum (Fig. S8). The resonances associated with H_α and H_β shift down- and upfield, respectively. The resonances of the TTF protons shift upfield, and are separated from two peaks into three. These changes in the spectra are characteristic[S5] of host-guest binding of TTF derivatives with $CBPQT^{4+}$.

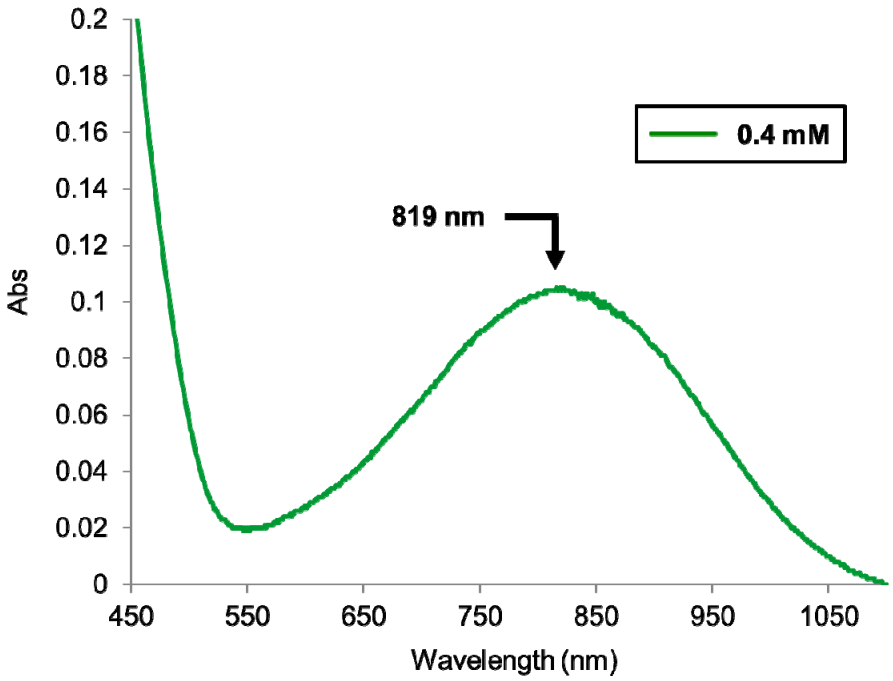

Figure S9: UV-Vis absorption spectrum (0.4 mM, 298K) of a 1:1 mixture of **S1** and **S2**•$4PF_6$.

The absorption band centered around 819 nm in the UV-Vis absorption spectrum (Fig. S9) of a mixture of **S1** and $CBPQT^{4+}$ is characteristic[S6] of charger-transfer between TTF and $CBPQT^{4+}$. The fact that the absorption maximum of **S1**⊂$CBPQT^{4+}$ is blue-shifted by about 35 nm as compared to TTF⊂$CBPQT^{4+}$ can be attributed to the conjugation of the acetylene with the TTF unit; some of the electron density from the TTF is delocalized into the triple bond.

S4. ^{1}H-^{1}H-g-DQF-COSY and ^{1}H-^{1}H ROESY Spectra of $\mathbf{1}^{4+}$

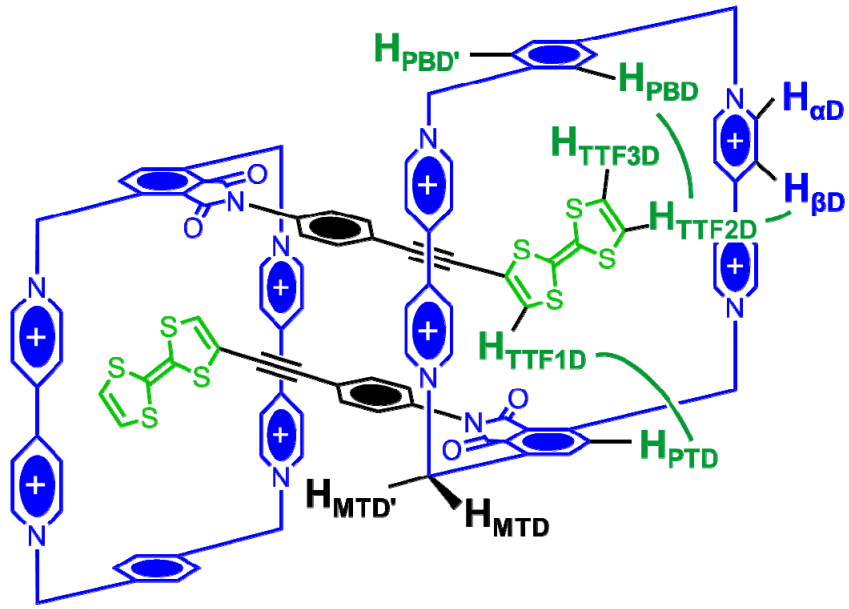

Figure S10: Proposed structure of the pseudo[c2]daisy chain dimer of two $\mathbf{1}^{4+}$ molecules. Important through-space interactions which can be identified in the ^{1}H-^{1}H-ROESY spectrum are indicated by green lines.

Low temperature (233 K) ^{1}H-^{1}H-g-DQF-COSY and ^{1}H-^{1}H ROESY spectra provide valuable insight into the proposed arrangement (Fig. S10) of the $\mathbf{1}^{4+}$ molecules when dimerised in the pseudo[c2]daisy chain form. In the COSY spectrum (Fig. S11), there are three sets of characteristic cross peaks. The peaks encircled by the blue box in Fig. S11 correspond to the through-bond interaction of $H_{\alpha D}$ and $H_{\beta D}$ protons of the bipyridinium units. There are four different $H_{\alpha D}$ and $H_{\beta D}$ resonances because the protons on either face of the CBPQT^{4+} unit are diastereotopic. The peaks encircled by the black box in Fig. S11 correspond to through-bond interactions of the methylene protons closest to the phthlamide unit, $H_{MTD'}$ and H_{MTD}. The resonances corresponding to $H_{MTD'}$ are shifted significantly upfield from H_{MTD}, presumably because of the shielding effects of the imide carbonyl lone pairs. H_{TTF3D} and H_{TTF2D} resonate at different frequencies because they are heterotopic. In the ROESY spectrum (Fig. S12), the significant cross peaks are of the opposite phase of the diagonal. H_{TTF2D} is engaged in through-space interactions – the cross peaks are encircled by green boxes in Fig. S12 – with (1) half of

the $H_{\beta D}$ protons, (2) the phenylene protons in $CBPQT^{4+}$, and (3) the H_{TTF1D} proton. It is important to note that we cannot determine what angle the phthalimide unit prefers to be in with respect to the $CBPQT^{4+}$ face from this data alone.

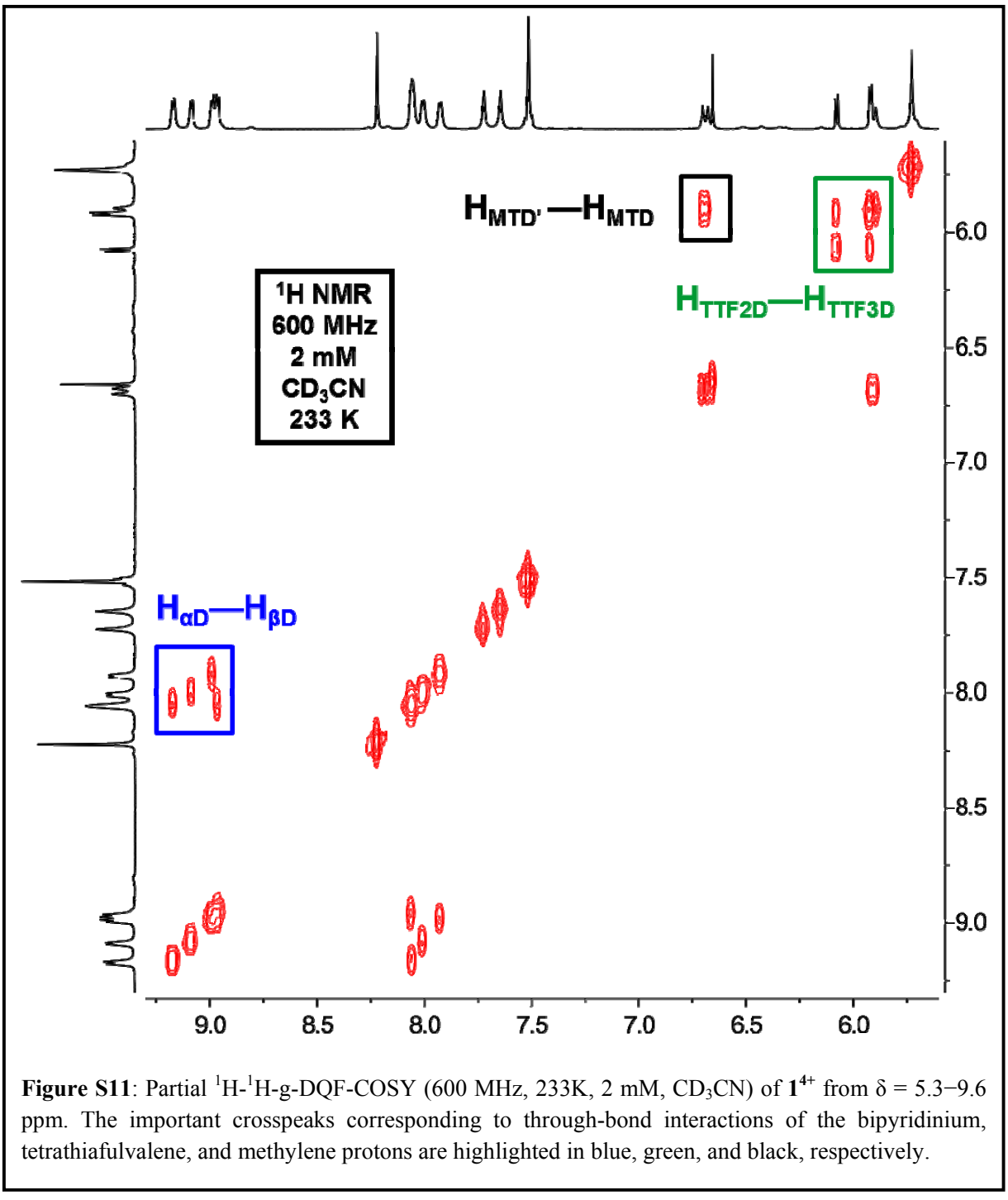

Figure S11: Partial ^{1}H-^{1}H-g-DQF-COSY (600 MHz, 233K, 2 mM, CD_3CN) of $\mathbf{1}^{4+}$ from δ = 5.3−9.6 ppm. The important crosspeaks corresponding to through-bond interactions of the bipyridinium, tetrathiafulvalene, and methylene protons are highlighted in blue, green, and black, respectively.

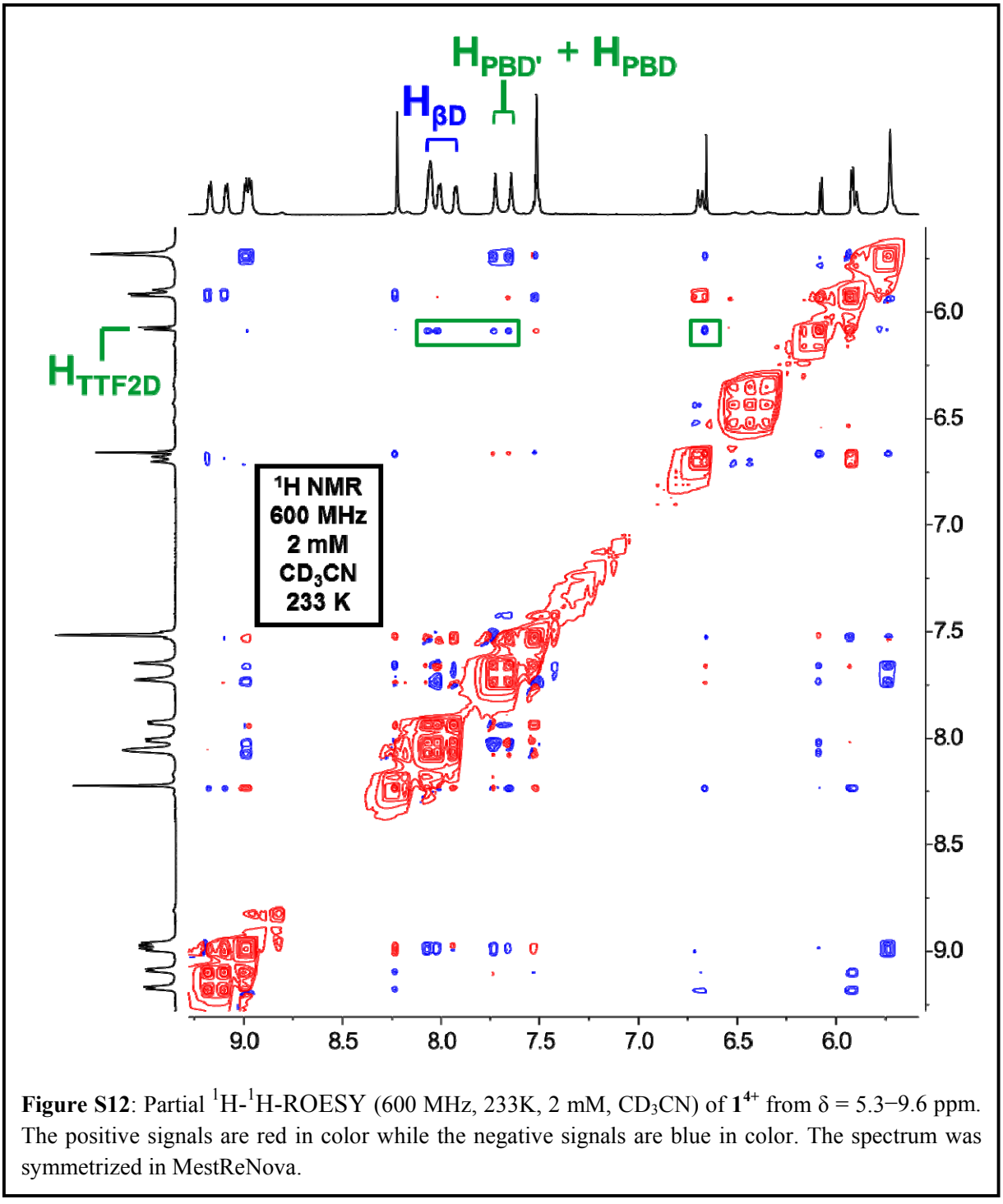

Figure S12: Partial ^{1}H-^{1}H-ROESY (600 MHz, 233K, 2 mM, CD_3CN) of $\mathbf{1}^{4+}$ from δ = 5.3−9.6 ppm. The positive signals are red in color while the negative signals are blue in color. The spectrum was symmetrized in MestReNova.

S5. UV-Vis Spectroscopy

A series of solutions of $\mathbf{1}^{4+}$ in MeCN ranging from 2.7 mM to 0.1 mM was prepared by diluting a 3.0 mM stock solution. The UV-Vis absorption spectra exhibited the expected decrease in

absorption as the concentration of the solution was lowered. When the Benesi-Hildebrand method was applied, a nonlinear curve was obtained, indicating that the CT band does not result from a simple host-guest complexation, but is rather most likely a consequence of an oligomerisation process, almost certainly dimerization.

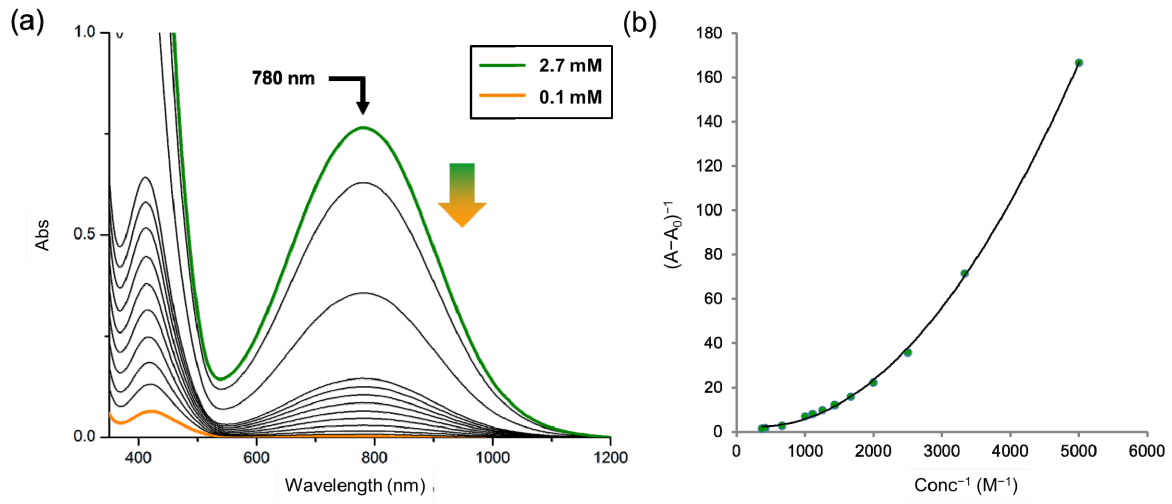

Figure S13: (a) Serial dilution UV-Vis absorption spectra (233 K, MeCN) of $\mathbf{1}^{4+}$. (b) Benesi-Hildebrand plot of the absorbances obtained from serial dilution. The black line serves as a trendline for the eye.

S6. References

S1. S. Kotha and R. J. Stoodley, *Bioorg. Med. Chem.*, 2002, **10**, 621−624.

S2. J. Riedl, P. Horáková, P. Šebest, R. Pohl, L. Havran, M. Fojta and M. Hocek, *Eur. J. Org. Chem.*, 2009, **2009**, 3519−3525.

S3. S. Fujii and J.-M. Lehn, *Angew. Chem., Int. Ed. Engl.*, 2009, **48**, 7635−7638.

S4. C.-H. Sue, S. Basu, A. C. Fahrenbach, A. K. Shveyd, S. K. Dey, Y. Y. Botros and J. F. Stoddart, *Chem. Sci.*, 2010, **1**, 119−125.

S5. M. B. Nielsen, J. O. Jeppesen, J. Lau, C. Lomholt, D. Damgaard, J. P. Jacobsen, J. Becher and J. F. Stoddart, *J. Org. Chem.*, 2001, **66**, 3359−3583.

S6. D. Philp, A. M. Z. Slawin, N. Spencer, J. F. Stoddart and D. J. Williams, *J. Chem. Soc. Chem. Commun.*, **1991**, 1584−1586.